

Spectral properties of oscillatory and non-oscillatory  $\alpha^2$ -dynamoes.

A. Giesecke, F. Stefani, G. Gerbeth

*Helmholtz-Zentrum Dresden-Rossendorf, Dresden, Germany**(Received 00 Month 200x; in final form 00 Month 200x)*

The eigenvalues and eigenfunctions of a linear  $\alpha^2$ -dynamo have been computed for different spatial distributions of an isotropic  $\alpha$ -effect. Oscillatory solutions are obtained when  $\alpha$  exhibits a sign change in the radial direction. The time-dependent solutions arise at so called exceptional points where two stationary modes merge and continue as an oscillatory eigenfunction with conjugate complex eigenvalues. The close proximity of oscillatory and non-oscillatory solutions may serve as the basic ingredient for reversal models that describe abrupt polarity switches of a dipole induced by noise.

Whereas the presence of an inner core with different magnetic diffusivity has remarkable little impact on the character of the dominating dynamo eigenmodes, the introduction of equatorial symmetry breaking considerably changes the geometric character of the solutions. Around the dynamo threshold the leading modes correspond to hemispherical dynamoes even when the symmetry breaking is small. This behavior can be explained by the approximate dipole-quadrupole degeneration for the unperturbed problem.

More complicated scenarios may occur in case of more realistic anisotropies of  $\alpha$ - and  $\beta$ -effect or through non-linearities caused by the back-reaction of the magnetic field (magnetic quenching).

*Keywords:* Dynamo, alpha-effect, mean-field-theory, oscillatory fields, reversal

## 1 Introduction

Oscillatory or reversing magnetic fields driven by a flow of an electrically conducting fluid are a well known astrophysical phenomenon. Thus the solar magnetic field regularly oscillates on a characteristic 22 yrs time scale whereas the dominating dipole component of the Earth's magnetic field irregularly changes its orientation every few 100 kyrs, conducting a so called reversal. Sign changes of the magnetic field also have been observed in the Cadarache von-Kármán-Sodium (VKS) dynamo, and depending on the difference of the rotation rates of the two flow driving impellers various regimes with oscillatory and/or chaotic behavior can be obtained (Berhanu *et al.* 2007). Whereas the time scale of the solar cycle can be reproduced using simple  $\alpha\Omega$ -dynamo models, an explanation of the observed equatorial migration requires further assumptions, e.g. meridional flow or negative radial shear at the surface. Regarding the geodynamo, three dimensional simulations of the magnetohydrodynamic equations as well as mean field models have been able to reproduce essential features of the Earth's magnetic field (Hoyng *et al.* 2002, Christensen 2011), but others, for example the very nature of the reversal mechanism or the large variation of reversal rates (McFadden and Merrill 1986) still are unsolved issues. A prominent feature of this paleomagnetic reversal frequency distribution is the occurrence of a few very long periods ( $\gtrsim 20$ Myrs) during which no reversal occurred at all (so called superchrons; Harland *et al.*, 1982). Another surprising but less known property are deviations of the distribution of inter-reversal time periods from an ideal Poisson distribution (Carbone *et al.* 2006, Sorriso-Valvo *et al.* 2007) indicating long term correlations in the reversal trigger mechanism(s).

In order to reliably disentangle internal reversal trigger mechanisms (e.g. intrinsic changes of the fluid flow pattern in the liquid outer core) from external sources (e.g. precession or changes in the heat flux through the core mantle boundary) numerical simulations are required that cover sufficient long time periods to allow for a large number of reversal events. In addition, numerical models should also be capable to incorporate the mechanisms that trigger individual reversals and reproduce general reversal

---

\*Corresponding author. Email: a.giesecke@hzdr.de

characteristics such as duration and field geometry during the actual reversal. Mean field models are ideally suited to execute long term simulations of the (mean field) induction equation because they are computational cheap. The price for this capability is a strong simplification by parameterizing induction effects of the turbulent small scale flow e.g. in terms of the  $\alpha$ -effect (Krause and Rädler 1980). Hence, any internal changes of the small scale turbulence (e.g. changes in statistical properties of the convection caused by gradual growth of the solid inner core) are suspected to encroach/expand into the comparably simple mean field coefficients. Nevertheless, mean field modelling of reversing magnetic fields has been remarkably successful (Hoyng *et al.* 2002, Stefani and Gerbeth 2005, Fischer *et al.* 2009). The present work is based on the idea that a polarity change is part of an oscillation of the dominant dipole mode (Stefani *et al.* 2007). A consequential model for irregularly occurring reversals requires a proximity of an oscillatory and a non-oscillatory branch so that a single transition between both states might be induced by noise. This is substantiated by the fact that polarity reversals in numerical dynamos are generally found in intermediate parameter regions between stable (dipolar) dynamos with small fluctuations and highly fluctuating and unstable dynamos (Olson and Christensen 2006).

The mean flow in the Earth's fluid core most probably is weak so that usual geodynamo models are based on an  $\alpha^2$  mechanism where an  $\alpha$ -effect (re-)generates the poloidal field from the poloidal field and vice versa. A general requirement for the occurrence of oscillating eigenmodes in  $\alpha^2$ -dynamos is  $\nabla\alpha \neq 0$  (Rädler and Bräuer 1987). However, for a long time it was assumed that the leading eigenmode in simple  $\alpha^2$ -dynamos is non-oscillatory and dominant oscillatory solutions are a curiosity that requires a rather elaborate configuration (Rüdiger *et al.* 2003). Recently, it has been discovered that oscillatory  $\alpha^2$ -dynamos are quite common when the radial profile of a spherically symmetric, isotropic  $\alpha$  exhibits a sign change (Stefani and Gerbeth 2003) and a stringent mathematical treatment of this model yields very general conditions for the occurrence of oscillating solutions (Günther *et al.* 2010). Meanwhile oscillating solutions have also been found in direct numerical simulations of thermal convection in a spherical shell (Schinnerer *et al.* 2011) or in a spherical wedge geometry with random helical forcing (Mitra *et al.* 2010). Such oscillating  $\alpha^2$ -dynamos might provide an alternative approach for the solar dynamo, e.g. the model of Mitra *et al.* (2010) exhibits equatorward migration without the requirement of meridional circulation or negative radial shear (which in the sun only occurs in a rather thin layer located close to the surface).

Here, we examine the behavior of axisymmetric eigenmodes generated in a two-dimensional kinematic  $\alpha^2$ -dynamo with isotropic  $\alpha$ -effect. The focus of our examinations is on the spectrum of eigenvalues in terms of growth rates and oscillation frequencies for two different radial profiles of the  $\alpha$ -effect. For this purpose we pick up the model of Giesecke *et al.* (2005a) where a sinusoidal radial  $\alpha$  distribution is assumed. We show that for this  $\alpha$ -distribution the leading modes around the dynamo threshold are oscillating independent of inner core conductivity or latitudinal perturbations that would provide an equatorial symmetry breaking. In extension to Giesecke *et al.* (2005a), where only the two dominating oscillating modes around the onset of dynamo action were discussed, here we investigate the emergence/disappearance of oscillating modes at so called exceptional points in more detail and briefly identify the fundamental differences in the radial structure of oscillatory and non-oscillatory eigenmodes. The work aims at building a bridge between original mean field models that have been developed in the sixties of the last Century, and recent results from observational and numerical approaches demonstrating the valuable impact of mean field theory for the development of a geodynamo reversal model.

## 2 Equations and Method

The basic assumption of the mean field approach is a separation of the velocity field  $\mathbf{u}$  and the magnetic field  $\mathbf{B}$  which are split into mean parts  $\langle \mathbf{u} \rangle$ ,  $\langle \mathbf{B} \rangle$  and fluctuating parts  $\mathbf{u}'$ ,  $\mathbf{B}'$  according to

$$\mathbf{B} = \langle \mathbf{B} \rangle + \mathbf{B}' \text{ and } \mathbf{u} = \langle \mathbf{u} \rangle + \mathbf{u}', \tag{1}$$

where  $\langle \cdot \rangle$  represents an appropriate space- and time average so that the Reynolds averaging rules apply. Then the temporal development of the mean magnetic field  $\langle \mathbf{B} \rangle$  is described by the mean field induction

equation

$$\partial_t \langle \mathbf{B} \rangle = \nabla \times (\langle \mathbf{u} \rangle \times \langle \mathbf{B} \rangle + \mathcal{E} - \eta \nabla \times \langle \mathbf{B} \rangle) \quad (2)$$

with the turbulent electromotive force (EMF)  $\mathcal{E} = \langle \mathbf{u}' \times \mathbf{B}' \rangle$  that describes the average induction action of (unresolved) small scale flow perturbations.  $\mathcal{E}$  results from the interaction of the fluctuating velocity field  $\mathbf{u}'$  with the mean magnetic field  $\langle \mathbf{B} \rangle$  and is formally represented by a linear functional of  $\langle \mathbf{u} \rangle$ ,  $\langle \mathbf{B} \rangle$  and the statistical properties of  $\mathbf{u}'$  (Krause and Rädler 1980). Assuming that the mean quantities vary only slightly around a certain space-time point, only contribution from a certain neighborhood must be taken into account and the EMF can be written as a Taylor expansion:

$$\mathcal{E}_i = \langle \mathbf{u}' \times \mathbf{B}' \rangle_i = \alpha_{ij} \langle B_j \rangle + \beta_{ijk} \frac{\partial \langle B_k \rangle}{\partial x_j} + \dots \quad (3)$$

where the coefficients  $\alpha_{ij}$  and  $\beta_{ijk}$  depend on the properties of the turbulent fluctuations  $\mathbf{u}'$ . In general, the turbulence is anisotropic so that  $\alpha$ - and  $\beta$ -effect are described by tensors of 2nd and 3rd rank, respectively. Here we restrict ourselves to the simplest case of isotropic turbulence so that  $\alpha$  and  $\beta$  are given by

$$\alpha_{ij} = \alpha_0 \delta_{ij}, \quad (4)$$

$$\beta_{ijk} = -\beta \epsilon_{ijk} \quad (5)$$

so that  $\alpha$  and  $\beta$  are prescribed by scalar quantities. Note that for a non-vanishing  $\alpha$ -effect the turbulence additionally must be non-mirrorsymmetric. With the definition of the turbulent diffusivity

$$\eta_T = \eta + \beta \quad (6)$$

and vanishing mean flow  $\langle \mathbf{u} \rangle = 0$  the mean field induction equation simplifies to an equation describing the temporal development of an  $\alpha^2$ -dynamo:

$$\partial_t \mathbf{B} = \nabla \times (\alpha \mathbf{B} - \eta_T \nabla \times \mathbf{B}) \quad (7)$$

(the brackets around the mean field  $\mathbf{B}$  from now on are dropped for simplicity). Equation (7) is linear in  $\mathbf{B}$  and the ansatz  $\mathbf{B} = \mathbf{B}(\mathbf{r})e^{\gamma t}$  leads to a linear eigenvalue problem

$$\mathcal{M} \mathbf{B} = \gamma \mathbf{B} \quad (8)$$

with the matrix  $\mathcal{M}$  containing the dynamo operator from the right hand side of (7), and the eigenvalue  $\gamma = \sigma + i\nu$  (growth rate  $\sigma$  and frequency  $\nu$ ). For uniform distributions of  $\alpha$  and  $\eta_T$  (semi-) analytic solutions are known (e.g. Krause and Rädler, 1980). For more complex flows and spatial distributions of  $\alpha$  and  $\eta$  a numerical solution of the eigenvalue problem is required (e.g. Roberts and Stix 1972, Dudley and James 1989). Here we solve (8) in a sphere surrounded by a non-conducting vacuum applying the method presented in Schrunner *et al.* (2010). The approach is based on the biorthogonality of the electric current  $\mathbf{j} = \mu_0^{-1} \nabla \times \mathbf{B}$  and the vector potential  $\mathbf{A}$  and explicitly utilizes an expansion of the magnetic field  $\mathbf{B}$  into (analytical known) free decay modes. The method allows a very fast computation of eigenvalues and eigenfunctions for nearly arbitrary spatial distributions of  $\alpha$  and/or  $\eta_T$ . Further we restrict our examination to the axisymmetric field which is dominating for isotropic  $\alpha$  and  $\beta$ . Higher azimuthal modes will be important in case of anisotropic  $\alpha$  coefficient (Tilgner 2004), although in case of anisotropic  $\eta_T$  axisymmetric modes become again dominant (Eltner and Rüdiger 2007).

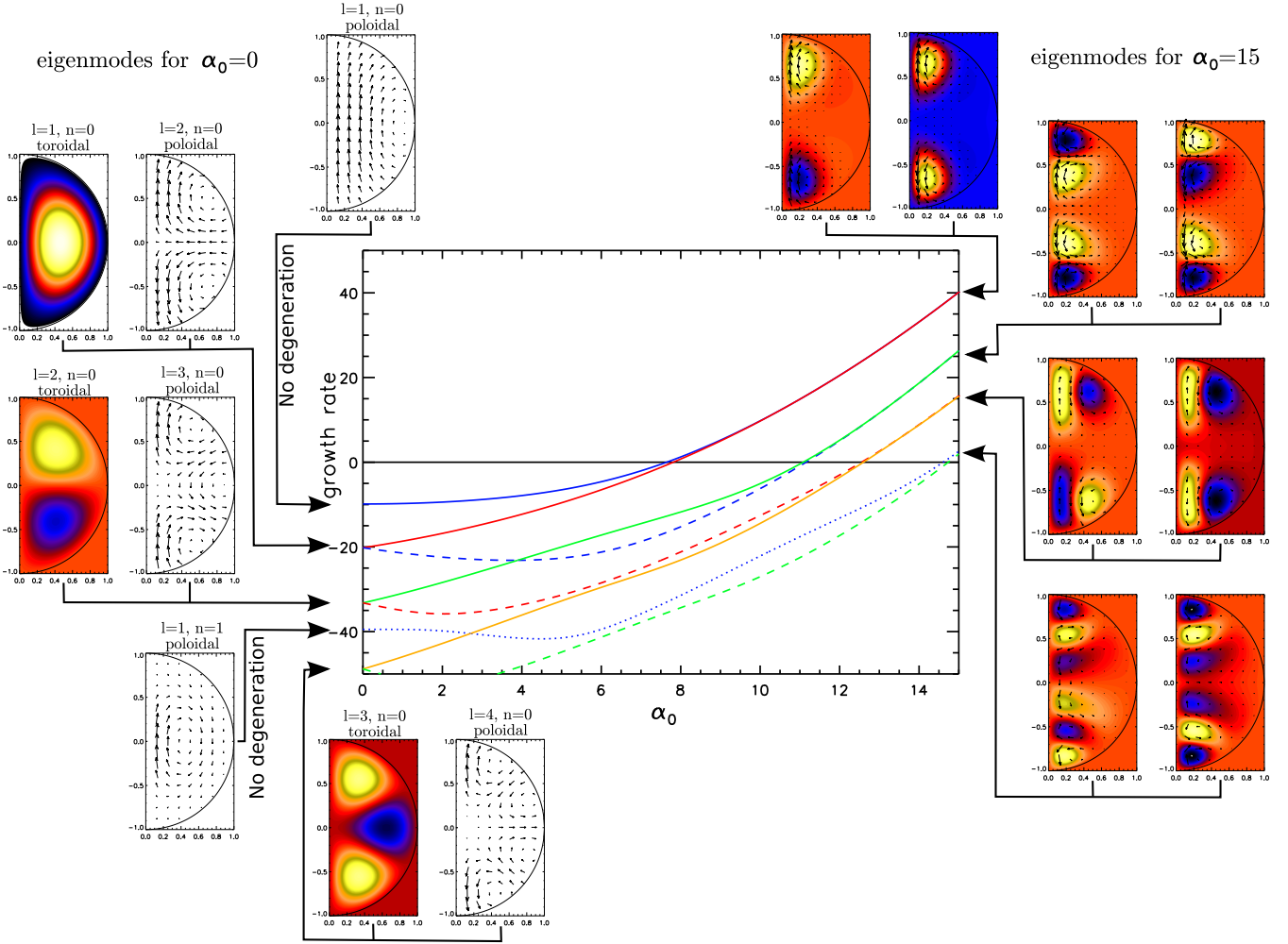


Figure 1. (colour online) Central panel: growth rates for an  $\alpha^2$  dynamo with  $\alpha = \alpha_0 \cos \vartheta$ . Note the transition between different types of degeneration when going from  $\alpha_0 = 0$  (free decay) to  $\alpha_0 \gg \alpha_{\text{crit}}$ . The small panels surrounding the central figure present the geometric structure of the eigenmodes for  $\alpha_0 = 0$  (left hand side) and for  $\alpha_0 = 15$  (right hand side). The colored contours denote the toroidal part and the arrows denote the poloidal part. Note the separation of toroidal and poloidal components in the free decay case ( $\alpha_0 = 0$ , left).

### 3 Results

We start with a full sphere (embedded in vacuum) where  $\alpha$  is created from turbulent motions in a convective layer subject to rotation. Then the EMF contains a term parallel to the mean magnetic field  $\mathcal{E} \propto (\mathbf{g} \cdot \boldsymbol{\Omega}) \mathbf{B}$  where  $\mathbf{g}$  points in the radial direction and  $\boldsymbol{\Omega}$  is parallel to the rotation axis ( $z$ -axis) so that  $(\mathbf{g} \cdot \boldsymbol{\Omega}) \propto \cos \vartheta$ . Thus, the  $\alpha$ -effect is maximum at the poles and vanishes at the equator:

$$\alpha = \alpha_0 \cos \vartheta. \quad (9)$$

This  $\alpha$  model has been examined e.g. in Roberts (1972). Here we revive these results and additionally present eigenvalues and eigenfunctions of higher order modes. The resulting spectrum of the leading dynamo eigenmodes in terms of the growth rates versus the amplitude  $\alpha_0$  is shown in figure 1.

All eigenvalues are real, i.e. all eigenfunctions are non-oscillatory modes. Due to the strict antisymmetry of  $\alpha$  with respect to the equator the parity of the eigenmodes remains preserved for increasing  $\alpha$ . That is, the  $\alpha$ -term in the induction equation couples toroidal and poloidal modes in a way that the dynamo eigenmode remains antisymmetric (in the following we call this "dipolar-like") or symmetric (in the following we call this "quadrupolar-like") with respect to the equator. At  $\alpha_0 = 0$  (free decay) an exact degeneration between "consecutive" modes is obtained (as indicated on the left side of figure 1). The degenerated eigenfunctions are always a pair of a purely toroidal and a purely poloidal mode which differ in multipolar

degree by  $\Delta l = 1$ . The degeneration vanishes for  $\alpha_0 > 0$  and around the dynamo threshold a slight predominance of the dipole mode occurs. The critical  $\alpha$  for the onset of dynamo action of the dipole mode ( $\alpha_0^{\text{crit}} = 7.645$ ) is close to the value for the quadrupolar mode ( $\alpha_0^{\text{crit}} = 7.813$ ). Both values agree with the results obtained by Roberts (1972) ( $\alpha_0^{\text{crit}} = 7.637$  for the dipole mode and  $\alpha_0^{\text{crit}} = 7.803$  for the quadrupole mode). For  $\alpha \gg \alpha_{\text{crit}}$  all eigenfunctions again approach a twofold degenerated state that consists of a pair of degenerated modes with similar geometric structure, but opposite equatorial symmetry (see right side in figure 1). The approximate degeneration between dipolar-like and quadrupolar-like modes is the result of a symmetry in the equations describing the  $\alpha^2$ -dynamo which is exact in case of perfect conducting boundary conditions. In that case dipolar eigenfunctions and quadrupolar eigenfunctions are adjoints of each other and thus have the same (conjugate) eigenspectrum (Proctor 1977). The degeneration is approximately retained in case of insulating boundary conditions so that the eigenvalues remain close to each other (Dobler and Rädler 1998).

**Radial dependence of  $\alpha$**  Next, we introduce a radial dependence for  $\alpha$  taken from the model presented in Giesecke *et al.* (2005a). This model utilizes an idealized parameterization in the radial direction that is based on local simulations of rotating magnetoconvection assuming conditions roughly suitable for the geodynamo (weak stratification, fast rotation, strong magnetic field; Giesecke *et al.*, 2005b). Qualitatively these simulations show that on the northern hemisphere  $\alpha$  is negative in the lower part of the liquid outer core and positive in the upper part, whereby the zero occurs roughly in the middle of the convective instable layer. The idealized radial  $\alpha$ -profile that incorporates these properties is given by

$$\alpha(\mathbf{r}) = \alpha_0 \cos \vartheta \sin \left( 2\pi \frac{(r - R_{\text{in}})}{(R_{\text{out}} - R_{\text{in}})} \right), \tag{10}$$

where the outer radius of the spherical domain is fixed to  $R_{\text{out}} = 1$  and  $R_{\text{in}}$  represents the radius of an inner core (see figure 2). A change in the radial profile was also considered in the first planetary mean field models (Steenbeck and Krause 1969). However, in that work  $\alpha$  was related to the radial derivative of the turbulence intensity  $u_{\text{rms}}^2$  and the authors exclusively looked for non-oscillating solutions.

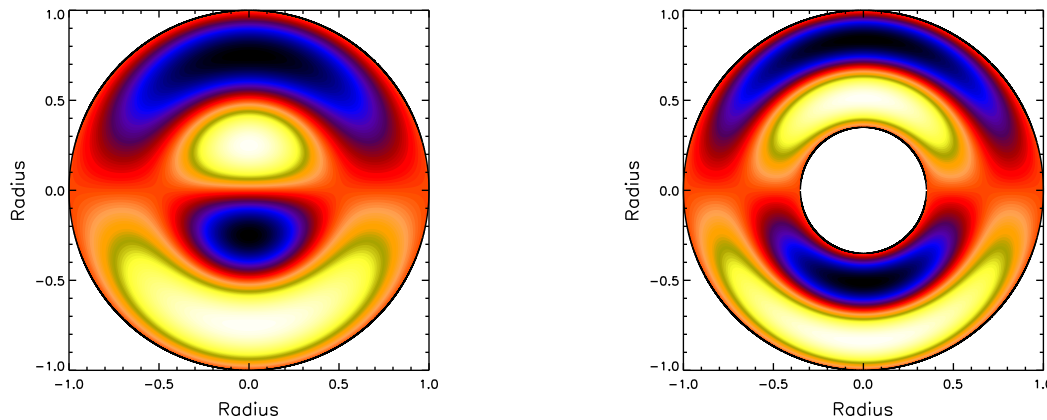


Figure 2. (colour online) Radial and latitudinal distribution of the  $\alpha$ -effect as given by (10). Left:  $R_{\text{in}} = 0$ ; Right:  $R_{\text{in}} = 0.35$  corresponding to the actual size of the Earth's inner core.

Here, we start assuming no inner core, i.e.  $R_{\text{in}} = 0$ . The spectrum for the leading axisymmetric modes is shown in figure 3. In contrast to the simple  $\alpha$ -profile examined in the previous section, oscillatory solutions (indicated by dotted curves) are obtained for this new radial  $\alpha$  profile. In particular, around the dynamo threshold the dominating eigenmodes are oscillatory dipolar-like (blue curve) and quadrupolar-like (red curve) solutions. The oscillating solutions appear/disappear at so called exceptional points (EP) where two stationary modes coalesce and continue as two oscillatory modes with conjugate complex eigenvalues, i.e. with the same growth rate and positive and negative frequency, respectively (the right panel of figure 3

shows only the positive frequency branch). Regarding the appearance of oscillatory modes at  $\alpha = 0$  (dotted

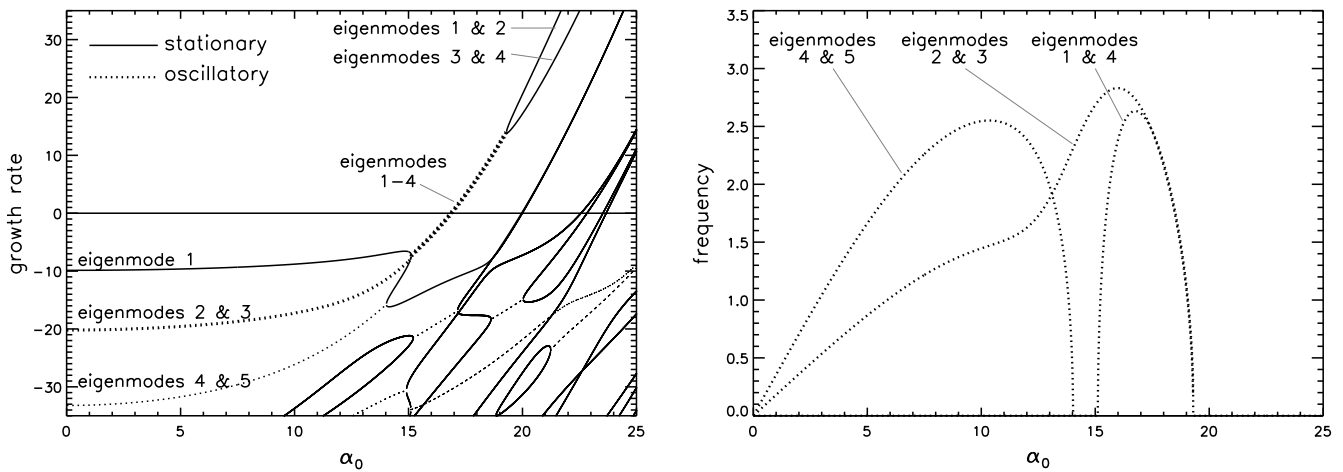


Figure 3. Left panel: growth rates versus  $\alpha_0$ . The leading eigenmodes are numbered in the order of their appearance at  $\alpha_0 = 0$ . Right panel: oscillation frequency versus  $\alpha_0$  (only the positive frequencies for the three leading time dependent modes are shown).

curves on the left panel of figure 3) it is necessary to stress that exactly at  $\alpha = 0$  (i.e. for free decay) these modes are stationary and degenerated, i.e.  $\alpha = 0$  is an exceptional point for these modes. The spectrum is far more complex than in models without any radial structure of the  $\alpha$ -effect and which is apparent by the confusing structure of the eigenvalues with a variety of level crossings and/or exceptional points where oscillatory solutions constitute or vanish. However, for  $\alpha \gg \alpha_{\text{crit}}$  predominantly stationary modes are observed.

**Decomposition in free decay modes** The change of the temporal character of the dynamo eigenmodes from non-oscillatory to oscillatory behavior is attended by a change in the radial structure. This can be seen by means of a decomposition of a dynamo eigenmode in terms of the leading free decay modes (which also represent the basis utilized in the numerical scheme). The dominating contributions in dependence on the magnitude of the  $\alpha$ -effect are shown in figure 4. For both symmetry classes the oscillatory regime

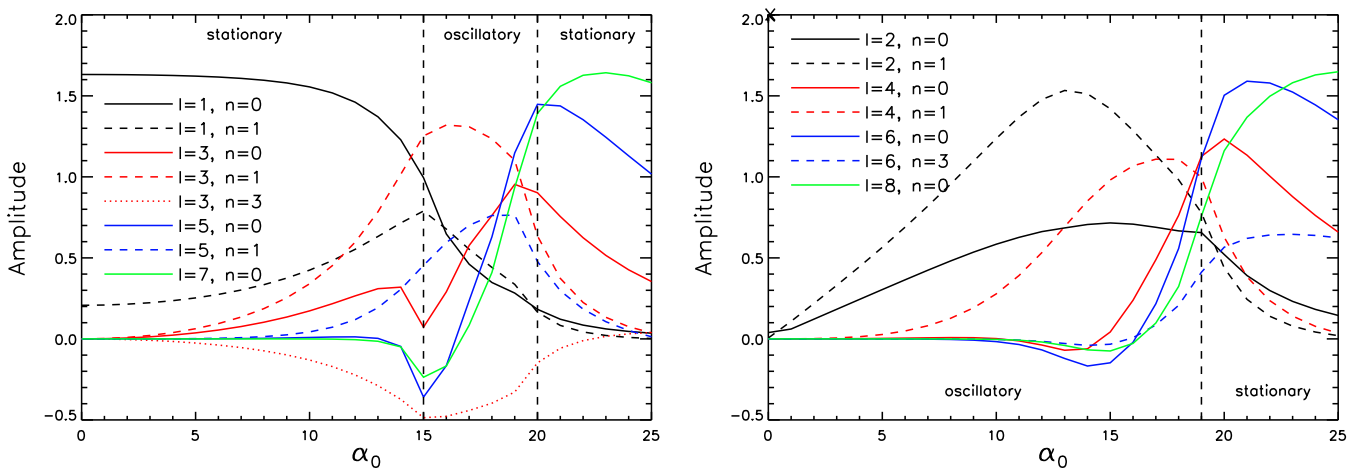


Figure 4. Contribution of characteristic free decay modes to the first dipolar-like dynamo eigenmode (left panel, eigenmode 1 in figure 3) and the first quadrupolar-like dynamo eigenmode (right panel, eigenmode 2 & 3 in figure 3).

is characterized by domination of modes with radial wavenumber  $n = 1$  whereas stationary solutions are

characterized by a domination of ( $n = 0$ ) modes<sup>1</sup>. Another feature shown in the decomposition of the dynamo eigenmode is the increment of the multipolar degree of the dominant contribution with increasing  $\alpha$ .

**Inner core** The influence of an inner core with finite electrical conductivity had been examined by Hollerbach and Jones (1993, 1995) and Wicht (2002) with surprisingly opposite conclusions. Whereas the latter only found little influence of finite inner core conductivity on temporal behavior of the dipole field, Hollerbach and Jones (1993, 1995) concluded from simulations that the finite conductivity of an inner core has a stabilizing impact and reversals could only occur if the field in the fluid outer core exhibits a large and long lasting fluctuation that allows the field to reverse throughout the inner core as well.

Figure 5(a) shows that the spectrum of the eigenmodes is only slightly changed when an inner core is considered with a radius  $R_{in} = 0.35$  and a uniform diffusivity within inner and outer core ( $\eta_T = 1$ ). The  $\alpha$ -effect is prescribed by the distribution (10) with  $\alpha = 0$  for  $r < R_{in}$ . The results for the same size of the inner core, but with a reduced diffusivity for  $r < R_{in}$ , is shown in figures 5(b) and (c). The introduction of an inner core without changing the diffusivity distribution has remarkable little influence on the spectrum (figure 5a) whereas a reduced inner core diffusivity for sufficiently small  $\alpha$  results in a split-up of the oscillatory modes into two stationary branches (figure 5b and c). However, around the onset of dynamo

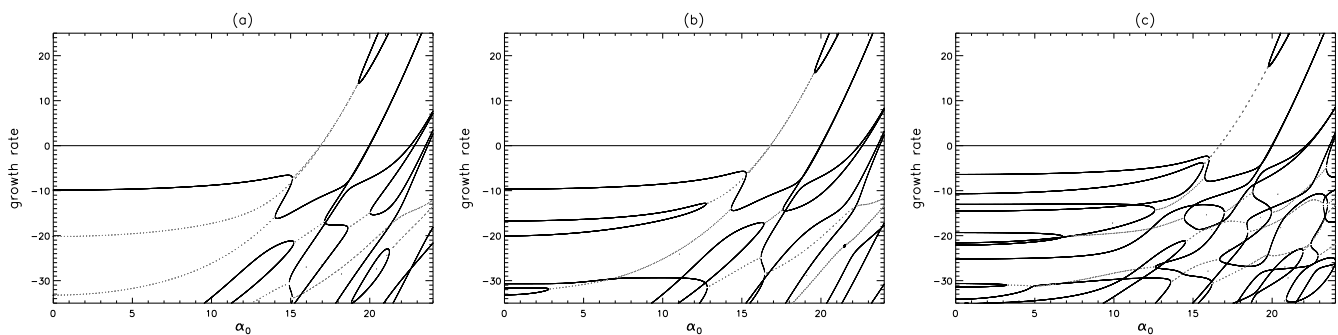


Figure 5. Growth rates versus  $\alpha_0$  for a modified  $\alpha$ -profile given by (10). An inner core is considered with an (earth-like) radius  $R_{in} = 0.35$  with a magnetic diffusivity  $\eta_{core} = 1, 0.5, 0.1$  (from left to right). Solid black curves represent non-oscillatory solutions and grey/dotted curves show oscillatory solutions.

action the typical pattern of the leading dynamo eigenmodes is hardly changed with increasing inner core conductivity. For example, the reduction from  $\eta_{core} = 1$  to  $\eta_{core} = 0.1$  leads only to a small decrease of the critical  $\alpha$ -magnitude from  $\alpha_{crit} \approx 16.9$  to  $\alpha_{crit} \approx 16.5$ . Furthermore, the temporal behavior of the leading modes is not changed within this regime, i.e. the leading modes remain oscillating around the onset of dynamo action independent of the inner core conductivity. In particular for  $\alpha \gg \alpha_{crit}$  no changes can be observed in the behavior of the leading modes. The main impact of an enhanced inner core conductivity is manifested in the cancellation of the degeneration of the eigenfunction for  $\alpha \lesssim \alpha_{crit}$ . Consequently, the spectrum becomes more complex than in case of no inner core or with uniform conductivity.

**Equatorial symmetry breaking** A coupling between dipole and quadrupole is the basis of the low dimensional reversal model of P  tr  lis and Fauve (2008), P  tr  lis *et al.* (2009) where the authors conclude that the reversal rate is constrained by breaking of the equatorial symmetry. With this motivation in the background, we investigate the influence of equatorial symmetry breaking of the  $\alpha$ -effect. In the model an additional term is added proportional to  $\cos(2\vartheta)$  leading to

$$\alpha = \alpha_0 \sin \left( \frac{2\pi (r - R_{in})}{R_{out} - R_{in}} \right) (\cos \vartheta + b \cos(2\vartheta)) \quad (11)$$

<sup>1</sup> $n$  characterizes the degree of a spherical Bessel function of a particular free decay mode and determines the radial behavior.

where  $b \ll 1$  and again  $R_{\text{in}} = 0.35$ . The main impact of the parameter  $b$  is a coupling of dipolar-like and quadrupolar-like modes so that a distinction in terms of parity with respect to the equator is no longer possible.

The resulting growth rates for various values of the parameter  $b$  are shown in figure 6 whereby  $\alpha$  is restricted to values around the dynamo threshold. Without symmetry breaking two oscillatory eigenfunc-

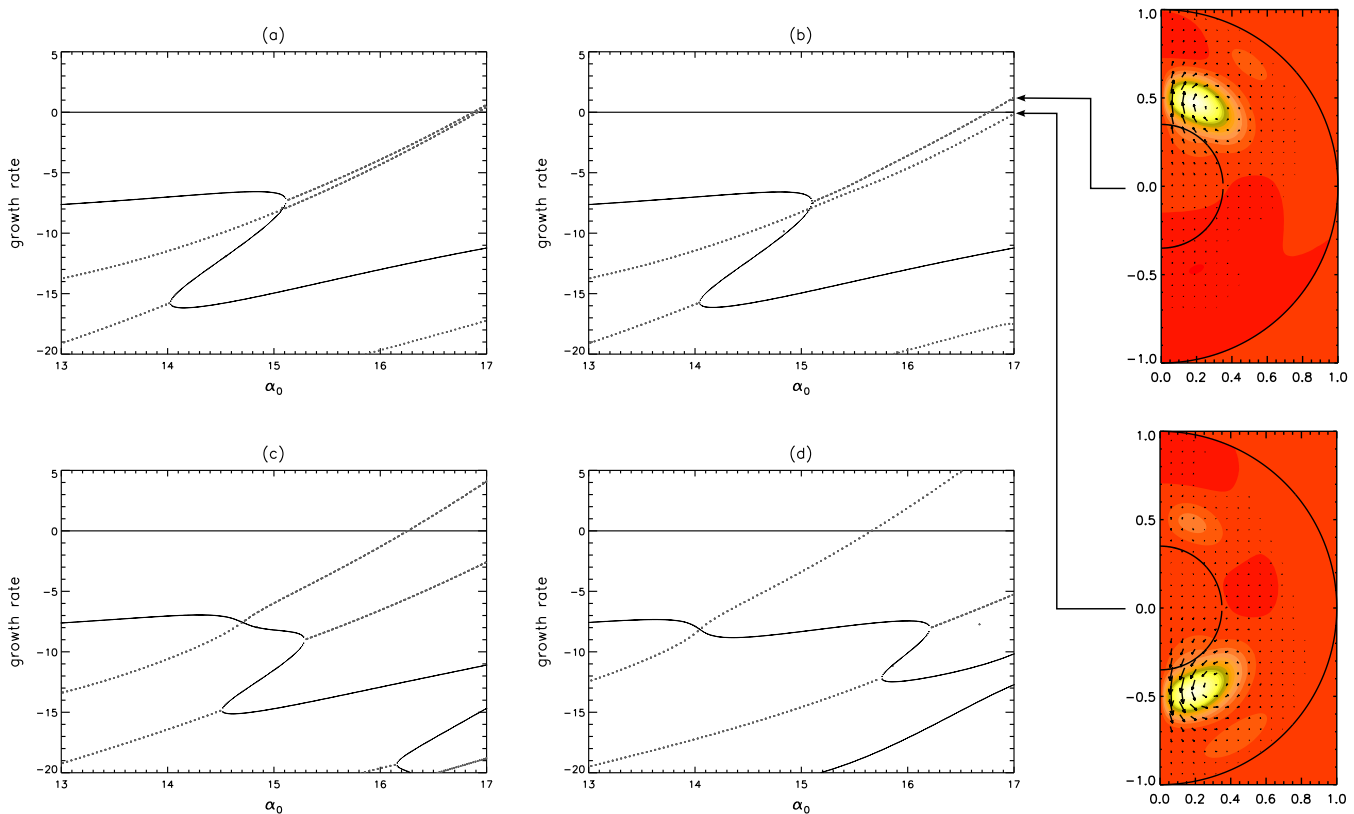


Figure 6. Extraction of growth rates vs.  $\alpha_0$  for dynamo models with equatorial symmetry breaking demonstrating the impact of symmetry breaking on the degeneration of the eigenfunctions. Solid curves denote stationary solutions and dotted curves denote oscillatory solutions.  $b = 0.00, 0.01, 0.05, 0.10$ . The contour plots on the right hand side show the pattern of the (hemispherical) eigenmodes for case (b) at  $\alpha_0 = 17$  (colour online).

tions that correspond to an oscillatory dipolar-like mode and an oscillatory quadrupolar-like mode cross the dynamo threshold around  $\alpha_0 \approx 16.9$ . The coupling of dipolar-like and quadrupolar-like modes results in a number of significant changes in the eigenvalues and geometric structure. Here we restrict the discussion to the behavior around the dynamo threshold of the leading eigenmode. First of all, we observe a reduction of the critical  $\alpha$  with increasing  $b$  which is attended by a breakup of the degeneration of the leading eigenmodes. However, the dominating eigenmodes retain their oscillatory property but due to the coupling of both symmetry classes a distinction into dipolar-like and quadrupolar-like eigenmodes is no longer possible. Compared to the undisturbed case, a considerable change in the field structure occurs for sufficiently strong  $\alpha$ . Around the dynamo threshold (and above) the coupling of both classes results in the occurrence of hemispherical dynamos that oscillate in time. Since dipolar-like and quadrupolar-like modes contribute roughly the same amount to the new coupled mode (recall that the growth rates of both types are roughly equal in the case without any perturbation) the coupled dynamo mode is concentrated within one hemisphere. Since dipolar and quadrupolar modes have a very similar structure, their contribution cancel out in one hemisphere so that magnetic energy is concentrated in the remaining hemisphere.

## 4 Conclusions

We have re-confirmed in a simple mean-field dynamo model that oscillatory  $\alpha^2$ -dynamoes are possible when the radial profile of  $\alpha$  exhibits a more complex structure. Our model is based on a particular radial profile of the  $\alpha$ -effect that behaves  $\propto \sin(r)$ . The choice of this profile is not arbitrary but is motivated by simulations of rotating magnetoconvection (Giesecke *et al.* 2005b) and quasi-linear computations performed by Soward (1974). On a first glance the occurrence of oscillatory solutions seems quite robust. Around the onset of dynamo action, growing oscillatory solutions dominate independently of core conductivity (and/or core size) or equatorial symmetry breaking. More important for a disappearance of oscillatory solutions might be deviations from the ideal sin-profile such as shifts of the zero crossing (Giesecke *et al.* 2005a) which has not been examined here.

The eigenfunctions of the  $\alpha^2$ -model exhibit a couple of remarkable properties that characterize the geometric structure of the eigenfields. In the oscillatory regime the eigenfunctions are dominated by contributions with higher radial wavenumber whereas the steady solutions essentially are determined by eigenfunctions with sparse radial structure. Hence, it is suggestive to look for an indication of a similar contribution of higher radial modes during an reversal in three-dimensional MHD simulations of the geodynamo or in field reconstructions from paleomagnetic observations as e.g. executed by Leonhardt and Fabian (2007).

For  $\alpha$ -distributions with perfect equatorial (anti-)symmetry  $\alpha \propto \cos\vartheta$  the dipolar and quadrupolar modes remain separated since no interaction between these modes is possible. The eigenmodes with different equatorial symmetry exhibit an approximate degeneration which would be exact in case of perfectly conducting boundary conditions. The corresponding proximity of growth rates for dipole and quadrupole has a dramatic impact when a small perturbation is considered that breaks the equatorial symmetry. In the vicinity of the dynamo threshold the resulting coupling between dipolar- and quadrupolar-like modes leads to hemispherical dynamo action. Indeed, the spatial reconstruction of the last reversal (the Matuyama-Brunhes transition  $\sim 780$  kyrs ago) shows a growing contribution of the quadrupolar component during the actual reversal (Leonhardt and Fabian 2007) but there are no hints for hemispherical dynamo action taken place in the Earth's core. Nevertheless, hemispherical dynamo action might have been the reason for the non-uniform crust magnetization as a result of the ancient martian dynamo (Landeau and Aubert 2011).

Our results differ from the achievement of Gallet and P  tr  lis (2009) who examined a kinematic  $\alpha^2$  model using a strongly localized  $\alpha$ -effect concentrated in two thin shells. In their model it is the coupling between dipole and quadrupole induced by equatorial symmetry breaking which leads to an oscillating eigenmode, whereas in our model the coupling between different radial modes (induced by the radial variation of  $\alpha$ ) is responsible for the oscillatory behavior. The simplicity of both models, however, prevents a robust conclusion which specific behavior indeed is realized in the geodynamo.

Regarding the Earth's magnetic field, a reason for the suppression of the quadrupole might arise from anisotropies of the turbulent flow essentially caused by the fast rotation of the Earth. These anisotropies resulting from the fast rotation of the Earth which suppresses variations/fluctuations along the rotation axis should be reflected in more realistic models of the  $\alpha$ -tensor as well as in the diffusivity tensor. Using more realistic anisotropic structure of the  $\alpha$ -tensor (but isotropic  $\eta$ ) results in domination of non-axisymmetric (i.e.  $m = 1$ ) modes (Giesecke *et al.* 2005a). This domination can be circumvented by assuming anisotropic description for  $\eta$  as well (Tilgner 2004). Note that non-axisymmetric modes indeed seem to be important in the reconstruction of the field pattern during the last reversal (the Matuyama-Brunhes transition) where the most important field contribution is determined by a  $m = 2$  contribution (Leonhardt and Fabian 2007).

A substantial limitation of the presented results is the linear character of the kinematic models, in particular regarding the proximity of the eigenvalues of leading dipolar and quadrupolar eigenmodes. Thus a robust prediction on the behavior in a saturated state is difficult and more elaborated mean field models will require the consideration of backreaction of the magnetic field by virtue of  $\alpha$ -quenching. Qualitatively, we expect a similar behavior as it has been described by Stefani and Gerbeth (2005) in a one-dimensional non-linear model of a reversing  $\alpha^2$ -dynamo. Assuming that the magnetic quenching of the  $\alpha$ -effect determines the instantaneous growth rate the authors showed that the corresponding eigenmode is

inevitably driven towards the oscillatory branch. This shift is attended by self accelerating field decay and the emerging local maximum of the growth rate in connection with noise provide the essential preconditions to switch from a stationary branch to an oscillatory branch and vice versa.

### Acknowledgments

Financial support from Deutsche Forschungsgemeinschaft (DFG) in frame of the Collaborative Research Center (SFB) 609 is gratefully acknowledged.

### REFERENCES

- Berhanu *et al.*, M., Magnetic field reversals in an experimental turbulent dynamo. *Europhys. Lett.* 2007, **77**, 59001–+.
- Carbone, V., Sorriso-Valvo, L., Vecchio, A., Lepreti, F., Veltri, P., Harabaglia, P. and Guerra, I., Clustering of polarity reversals of the geomagnetic field. *Phys. Rev. Lett.* 2006, **96**, 128501–+.
- Christensen, U.R., Geodynamo models: Tools for understanding properties of Earth's magnetic field. *Phys. Earth Planet. Int.* 2011, **187**, 157–169.
- Dobler, W. and Rädler, K.H., An integral equation approach to kinematic dynamo models. *Geophys. Astrophys. Fluid Dyn.* 1998, **89**, 45–74.
- Dudley, M.L. and James, R.W., Time-dependent kinematic dynamos with stationary flows. *Phil. Trans. R. Soc. Lond. A* 1989, **425**, 407–429.
- Elstner, D. and Rüdiger, G., How can  $\alpha^2$ -dynamos generate axisymmetric magnetic fields?. *Astron. Nachr.* 2007, **328**, 1130–1132.
- Fischer, M., Gerbeth, G., Giesecke, A. and Stefani, F., Inferring basic parameters of the geodynamo from sequences of polarity reversals. *Inverse Probl.* 2009, **25**, 065011.
- Gallet, B. and Pétrélis, F., From reversing to hemispherical dynamos. *Phys. Rev. E* 2009, **80**, 035302–+.
- Giesecke, A., Rüdiger, G. and Elstner, D., Oscillating  $\alpha^2$ -dynamos and the reversal phenomenon of the global geodynamo. *Astron. Nachr.* 2005a, **326**, 693–700.
- Giesecke, A., Ziegler, U. and Rüdiger, G., Geodynamo  $\alpha$ -effect derived from box simulations of rotating magnetoconvection. *Phys. Earth Planet. Int.* 2005b, **152**, 90–102.
- Günther, U., Langer, H. and Tretter, C., On the spectrum of the magnetohydrodynamic mean-field  $\alpha^2$ -dynamo operator. *SIAM J. Math. Anal.* 2010, **42**, 1413–1447.
- Harland, W., Cox, A., Liewellyn, P., Pickton, C., Smith, A. and Walters, R., *A geological time scale*, 1982 (Cambridge University Press).
- Hollerbach, R. and Jones, C.A., Influence of the Earth's inner core on geomagnetic fluctuations and reversals. *Nature* 1993, **365**, 541–543.
- Hollerbach, R. and Jones, C.A., On the magnetically stabilizing role of the Earth's inner core. *Phys. Earth Planet. Int.* 1995, **87**, 171–181.
- Hoyng, P., Schmitt, D. and Ossendrijver, M.A.J.H., A theoretical analysis of the observed variability of the geomagnetic dipole field. *Phys. Earth Planet. Int.* 2002, **130**, 143–157.
- Krause, F. and Rädler, K.H., *Mean-field magnetohydrodynamics and dynamo theory*, 1980 (Oxford: Pergamon Press).
- Landeau, M. and Aubert, J., Equatorially asymmetric convection inducing a hemispherical magnetic field in rotating spheres and implications for the past martian dynamo. *Phys. Earth Planet. Int.* 2011, **185**, 61–73.
- Leonhardt, R. and Fabian, K., Paleomagnetic reconstruction of the global geomagnetic field evolution during the Matuyama/Brunhes transition: Iterative Bayesian inversion and independent verification. *Earth Planet. Sci. Lett.* 2007, **253**, 172–195.
- McFadden, P.L. and Merrill, R.T., Geodynamo energy source constraints from palaeomagnetic data. *Phys. Earth Planet. Int.* 1986, **43**, 22–33.

- Mitra, D., Tavakol, R., Käpylä, P.J. and Brandenburg, A., Oscillatory Migrating Magnetic Fields in Helical Turbulence in Spherical Domains. *Astrophys. J. Lett.* 2010, **719**, L1–L4.
- Olson, P. and Christensen, U.R., Dipole moment scaling for convection-driven planetary dynamos. *Earth Planet. Sci. Lett.* 2006, **250**, 561–571.
- Pétrélis, F. and Fauve, S., Chaotic dynamics of the magnetic field generated by dynamo action in a turbulent flow. *J. Phys. Condens. Matter* 2008, **20**, 4203.
- Pétrélis, F., Fauve, S., Dormy, E. and Valet, J.P., Simple mechanism for reversals of Earth’s magnetic field. *Phys. Rev. Lett.* 2009, **102**, 144503–+.
- Proctor, M.R.E., On the eigenvalues of kinematic alpha-effect dynamos. *Astron. Nachr.* 1977, **298**, 19–25.
- Rädler, K.H. and Bräuer, H.J., On the oscillatory behaviour of kinematic mean-field dynamos. *Astron. Nachr.* 1987, **308**, 101–109.
- Roberts, P.H., Kinematic dynamo models. *Phil. Trans. R. Soc. Lond. A* 1972, **272**, 663–698.
- Roberts, P.H. and Stix, M., AC-effect dynamos, by the Bullard-Gellman formalism. *Astron. Astrophys.* 1972, **18**, 453.
- Rüdiger, G., Elstner, D. and Ossendrijver, M., Do spherical  $\alpha^2$ -dynamos oscillate?. *Astron. Astrophys.* 2003, **406**, 15–21.
- Schrinner, M., Petitdemange, L. and Dormy, E., Oscillatory dynamos and their induction mechanisms. *Astron. Astrophys.* 2011, **530**, A140.
- Schrinner, M., Schmitt, D., Jiang, J. and Hoyng, P., An efficient method for computing the eigenfunctions of the dynamo equation. *Astron. Astrophys.* 2010, **519**, A80+.
- Sorriso-Valvo, L., Stefani, F., Carbone, V., Nigro, G., Lepreti, F., Vecchio, A. and Veltri, P., A statistical analysis of polarity reversals of the geomagnetic field. *Phys. Earth Planet. Int.* 2007, **164**, 197–207.
- Soward, A.M., A convection-driven dynamo: I. The weak field case. *Phil. Trans. R. Soc. Lond. A* 1974, **275**, 611–646.
- Steenbeck, M. and Krause, F., On the Dynamo Theory of Stellar and Planetary Magnetic Fields. II. DC Dynamos of Planetary Type. *Astronomische Nachrichten* 1969, **291**, 271–286.
- Stefani, F. and Gerbeth, G., Oscillatory mean-field dynamos with a spherically symmetric, isotropic helical turbulence parameter  $\alpha$ . *Phys. Rev. E* 2003, **67**, 027302–+.
- Stefani, F. and Gerbeth, G., Asymmetric polarity reversals, bimodal field distribution, and coherence resonance in a spherically symmetric mean-field dynamo model. *Phys. Rev. Lett.* 2005, **94**, 184506–+.
- Stefani, F., Xu, M., Sorriso-Valvo, L., Gerbeth, G. and Günther, U., Oscillation or rotation: a comparison of two simple reversal models. *Geophys. Astrophys. Fluid Dyn.* 2007, **101**, 227–248.
- Tilgner, A., Small scale kinematic dynamos: beyond the  $\alpha$ -effect. *Geophys. Astrophys. Fluid Dyn.* 2004, **98**, 225–234.
- Wicht, J., Inner-core conductivity in numerical dynamo simulations. *Phys. Earth Planet. Int.* 2002, **132**, 281–302.